

Application of near-infrared responsive nano-carrier for controlled drug delivery: synthesis, isotherm and kinetic studies

M. Mahdavijalal¹, H. Ahmad Panahi^{1,*}, A. Niazi¹, A. Tamaddon¹, E. moniri²

1- Department of Chemistry, Central Tehran Branch, Islamic Azad University, Tehran, Iran

2- Department of Chemistry, Varamin (Pishva) Branch, Islamic Azad University, Varamin, Iran

* Corresponding author email: h.ahmadpanahi@iauctb.ac.ir

Received: Oct. 12, 2021, Revised: Oct. 26, 2021, Accepted: Dec. 26, 2021, Available Online: Mar. 12, 2022

DOI: 10.30495/ijbbo.2021.689781

ABSTRACT—Due to the importance of selecting an appropriate strategy in drug delivery systems, numerous studies have been performed to support this process. However, there are still major obstacles associated with the targeted drug delivery to cancer tissues. Hence, the main focus of this study is to develop the current cancer therapies by using drug delivery systems. To achieve this goal, we have synthesized a near-infrared light responsive drug carrier based on WS₂ nano-sheets, which can be a good candidate for applications such as drug delivery vehicle and chemo-photothermal treatments. In this study, a rapid and economy synthesis method was employed to modify the nano-sheets of WS₂ for targeted drug delivery of bicalutamide as a prostate anti-cancer drug. The investigation of adsorption isotherm was fitted well by Langmuir model ($q_{max} = 15.87 \text{ mg g}^{-1}$). The evaluation of adsorption kinetic was better expressed by pseudo-second-order kinetic model ($R^2=0.9998$). In-vitro drug release study was performed more rapid and complete in simulated blood fluid (pH=7.4) at 50°C than 37°C. Besides, the activity of the produced nano-carrier was examined under near-infrared light irradiation (at 808 nm). The drug release data were investigated through Zero-order, First-order, Higuchi, Hixson-Crowell and Korsmeyer–Peppas mathematical models.

KEYWORDS: Thermo-sensitive polymer, Drug delivery, Bicalutamide, In-vitro drug release, WS₂ nano-sheets, Near-infrared light irradiation.

I. INTRODUCTION

Prostate cancer is a common disease of the prostate gland and rising worldwide burden of this disease has threatened patients and health-care systems in most countries [1]. Mainly, pharmaceutical compounds including bicalotamide, flutamide, and nilotamide are most widely used as inhibitors in the treatment of prostate cancer in men. Among these pure anti-androgens, bicalutamide (BLT) takes more advantages than others as it possesses a long half-life and tolerable side effects. On the other hand, BLT has a low bioavailability due to its poor water solubility ($<50 \mu\text{g/mL}$ at pH 7.4 and 37°C) as an oral non-steroidal anti-androgen [2]. In recent years, the development of drug delivery systems using nanotechnology by the researchers has led to improved therapeutic

effects of drugs. Indeed, nano-carriers as drug vehicles can improve the overall therapeutic efficacy of anti-cancer agents by changing the biological situation and increasing the bioavailability of therapeutic drugs. Such a nano-therapy system with selective accumulation in tumor tissue would be an attractive approach to decrease the side effects and toxicity of current cancer treatments [3]. To date, different nano-carriers with the aim of enhancing drug delivery efficiency and reducing off-target effects have been employed in drug delivery systems, including inorganic nanoparticles, micelles, liposomes, carbon nanotube, and magnetic nanoparticles [4-8]. Among these nano-materials, many encouraging outcomes have been reported from the polymeric nano-carriers in targeted delivery of anti-cancer drugs.

In this regard, two-dimensional transition metal dichalcogenide nano-materials such as MoS₂ and WS₂ have attracted tremendous attention of the scientists due to fully meeting of the requirements for drug delivery systems, including the high surface-to-volume ratio, optical properties, low toxicity, and suitable biocompatibility [9]. Indeed, the WS₂ nano-sheets can be employed not only as a nano-carrier for chemotherapy agents due to their sheet-shaped structure in drug delivery systems but also as an NIR absorbing agent for photothermal therapy. In this study, a rapid and novel strategy was employed to modify the WS₂ nano-sheets surfaces through the polymer grafting to increase the drug loading capacity. Specifically, poly (N-vinylcaprolactam) (PNVCL) as a thermo-sensitive polymer was incorporated into the synthesized polymer networks. In practice, the release of the drug by the produced nano-carrier should trigger by the significant response of the synthesized polymer networks to the stimulus. In this article, we explored the effect of NIR light irradiation on BLT release process using the produced nano-carrier. It is well accepted that the nano-sheets of WS₂ are hydrophilic and offer advantage of strong light absorption in the broad near-infrared wavelength region (800–1,200 nm) [10]. It is natural to anticipate that the light-to-heat conversion by the WS₂ nano-sheets, leads to the wrinkle of the thermo-sensitive polymer networks onto the WS₂ nano-carrier. This implies that by prolonging the laser time and subsequent increasing the temperature of the nano-sheets, the shrinkage in the polymer chains with PNVCL, releases BLT from the sites.

In this paper, a WS₂-based NIR responsive nano-carrier for in vitro controlled release of BLT was reported to develop the current cancer therapies in drug delivery systems. The surface of the WS₂ nano-sheets was directly modified by simple and economy chemical methods. Following, the thermo-sensitive polymer anchored to the grafted polymer chains. The polymer structure and morphology of the synthesized nano-carrier and also its ability to safely load and release of drug in a controlled manner were carefully explored. Accordingly,

in vitro drug release studies of the final nano-carrier was examined at two different temperature (T=37°C, T=50°C) at pH 7.4. Additionally, the photo-thermal activity of the optimum nano-carrier was investigated under near-infrared light (NIR) irradiation (at 808nm, 1.0 W/cm²). The drug adsorption process was evaluated by several well-known kinetics and isotherms models. Besides, the drug release data were examined by using Zero-order, First-order, Korsmeyer–Peppas, and Higuchi mathematical models.

II. EXPERIMENTAL SECTIONS

A. Reagents and solutions

Tungsten disulfide (WS₂), poly (N-vinylcaprolactam), allylamine (AAM)(C₃H₇N), 2,2 azobisisobutyronitrile (AIBN)(C₈H₁₂N₄), ethanol, methanol, allyl acetoacetate (AAAc)(C₇H₁₀O₃), acetonitrile, and trifluoroacetic acid (TFA)(C₂HF₃O₂) were purchased from Merck (Darmstadt, Germany). Magic buffer solutions were prepared to adjust solutions pH in the range of 3-8.

B. Instrumentation

The drug release was analyzed by Ultraviolet-visible (UV/Vis) spectrum (Perkin Elmer/Lambda 25 (Carolina- Williamston-USA). Field-emission scanning electron microscope (FESEM, Mira3-TESCAN, Czech Republic) was employed to evaluate the samples morphology parallel to elemental analysis with energy-dispersive X-ray spectrometer (EDAX). Near-infrared light device was ASHA beam laser diodes (at 808 nm wavelength, 1W/cm²) (Iran).

C. Modification of WS₂ nano-sheets surface

In this synthesis, WS₂ nano-sheets (2 g), AAAc (10 mL), PNVCL (0.8 g), AIBN (0.1g), and ethanol (40 mL) were added into a 250mL two-necked flask. The final mixture was refluxed for 7 h at 65°C under nitrogen atmosphere in a water bath [11]. Finally, the solid phase was collected with a centrifuged device (at 6000 rpm) and washed with ethanol (40 mL).

D. *Coupling of AAT with WS₂/AAE/PNVCL*

In this reaction, the precipitate obtained in the section 2.3 was dispersed in methanol (150 mL) and AAm (10 mL) was rapidly added into the solution. The mixture was refluxed for 7h at room temperature. Following, the contents of flask was centrifuges for 15 min and the solid precipitated was dried at room temperature.

E. *Formation of polymer network onto WS₂ nano-sheets*

To synthesize the final nano-carrier, the chemicals listed in section 2.3 along with the precipitate obtained (in section 2.4) were added into a 250 mL flask. The reaction was continued under the nitrogen atmosphere for 7 h at 65°C in a water bath [11]. Eventually, the produced smart modified nano-carrier (SMNC) was separated from the solution with a centrifuge device (at 7000 rpm) and dried at room temperature. Performance of the synthesized SMNC exposed to the NIR irradiation is shown in Fig. 1.

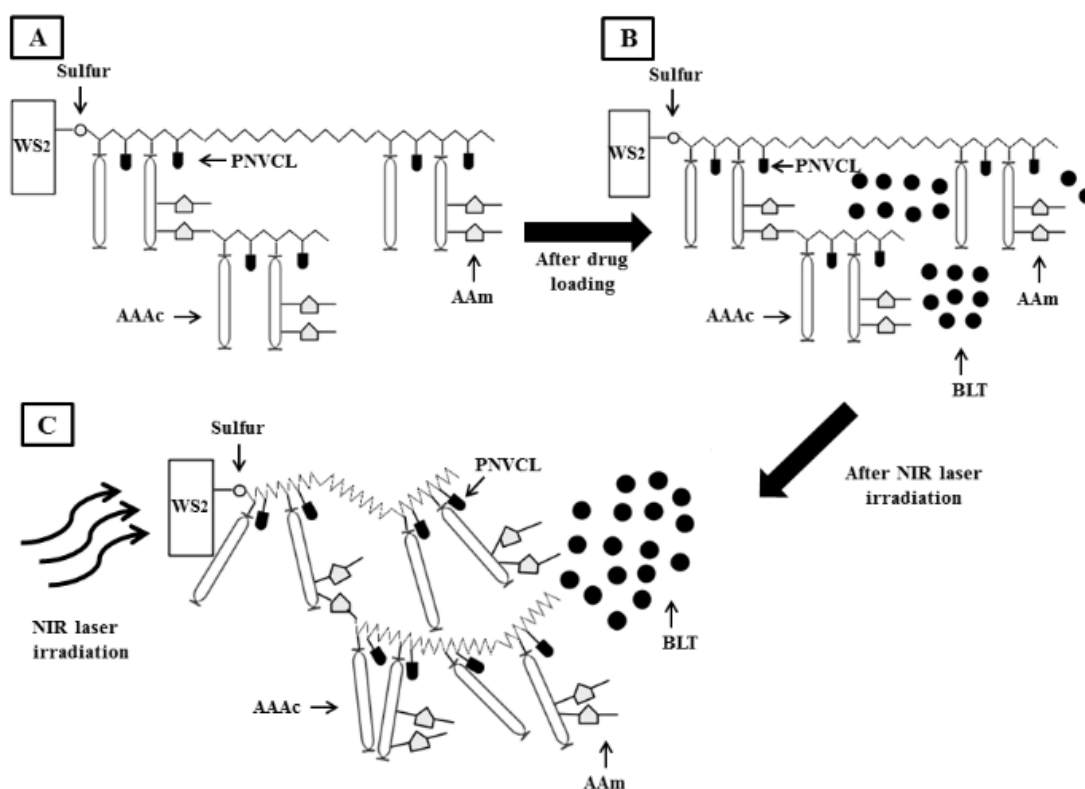


Fig. 1 Conceptual view of the SMNC performance exposed to NIR light irradiation: (A) The synthesized SMNC, (B) Surface adsorption of BLT by the synthesized SMNC, (C) BLT release process using the NIR laser irradiation (at 808 nm, 1.0 W cm⁻²).

F. *Drug loading and release process*

Batch experiments were performed with a known number of the micro-tubes filled with BLT solution (1.5 mL, 20 μg mL⁻¹) along with

10 mg of the synthesized SMNC under optimal conditions. The sealed micro-tubes were vortexed for 10 min (at 25 °C) and centrifuged at 7000 rpm (15 min). Finally, the concentration of BLT in each micro-tube was analyzed by the

UV-vis spectrophotometer (at 270 nm). To calculate the adsorbed BLT rate by the nano-carrier, following equation was used.

$$q_e = \frac{(c_0 - c_e)v}{M} \quad (1)$$

In Eq. (1), q_e (mg g^{-1}) shows the equilibrium adsorption capacity, C_0 and C_e are the initial and equilibrium concentrations of BLT in $\mu\text{g mL}^{-1}$, M (g) states the mass of the used SMNC and V (L) is solution volume.

G. Adsorption isotherms models

In this study, the mechanism of BLT adsorption by the produced SMNC nano-carrier was explored by using four famous adsorption isotherm models including Langmuir (Eq. 2), Freundlich (Eq. 3), Temkin (Eq. 4), and Redlich–Peterson (Eq. 5) were studied [12-15]. These studies were carried out by adding 10 mg of the synthesized nano-carrier into a series of micro-tubes with BLT solution (1.5 mL) at different concentrations (2, 5, 10, 15, 20, 30 and 40 $\mu\text{g mL}^{-1}$) under optimal conditions. The BLT adsorption data were computed by using the Eq. (1) and described by the adsorption isotherms models.

$$\frac{C_e}{q_e} = \left(\frac{1}{q_{\max} K_L} \right) + \left(\frac{C_e}{q_{\max}} \right) \quad (2)$$

$$\ln q_e = \ln K_F + \frac{1}{n} \ln C_e \quad (3)$$

$$q_e = \frac{RT}{b} \ln A + \frac{RT}{b} \ln C_e \quad (4)$$

$$\ln \left(A \frac{C_e}{q_e} - 1 \right) = g \ln (C_e) + \ln(B) \quad (5)$$

In Langmuir model, C_e (mg L^{-1}) denotes the equilibrium concentration of BLT; q_e (mg g^{-1}) represents the equilibrium adsorption capacity

of BLT; K_L (L mg^{-1}) is the Langmuir constant; and q_{\max} (mg g^{-1}) shows the adsorbed BLT weight, respectively. In Freundlich model, K_F (L g^{-1}) is the Freundlich constant and $1/n$ shows intensity of adsorption. In the Temkin model, A (L g^{-1}) is Temkin constant and B shows heat of drug uptake. In Redlich–Peterson model, A and B are the Redlich–Peterson constants and g states the heterogeneity of the nano-carrier, which lies between 0 and 1.

H. Adsorption kinetics models

The kinetics of BLT adsorption by the produced nano-carrier was investigated at different contact times. For this, six micro-tubes containing BLT solution (1.5 mL, 20 $\mu\text{g mL}^{-1}$) along with the produced nano-carrier were prepared. The samples were vortexed at the predetermined contact times (0–60min). Ultimately, the amount of the remained BLT in each supernatant was determined via the UV–Vis spectrophotometer. The results data were evaluated by three adsorption kinetic models namely, pseudo-first-order kinetic (Eq. 6), pseudo-second-order (Eq. 7), and the intra-particle diffusion model of Weber and Morris (Eq. 8) [16-18].

$$q_t = q_e (1 - e^{-k_1 t}) \quad (6)$$

(pseudo – first – order equation)

$$q_t = \frac{K_2 q_e^2 t}{1 + K_2 q_e t} \quad (7)$$

(pseudo – second – order equation)

$$q_t = K_i t^{0.5} + C_i \quad (8)$$

(intra – particle diffusion equation)

Where q_e (mg g^{-1}) is the adsorbed BLT rate and q_t (mg g^{-1}) is the equilibrium BLT rate. C_i (mg g^{-1}) shows the thickness of boundary layer. Besides, the constants of the kinetic models are shown as follows: k_1 (min^{-1}), K_2 ($\text{g mg}^{-1} \text{min}^{-1}$), and K_i ($\text{mg g}^{-1} \text{min}^{-1/2}$).

I. *In vitro drug release and kinetic modeling of drug release*

BLT in vitro release experiments were examined in simulated body fluids (phosphate buffered saline) at pH 7.4 through dialysis method. To do this, 300 mg of the loaded nano-carrier with BLT was put separately inside two dialysis bags (MWCO 12,000–14,000, Sigma, Germany). The bags were immersed in two separate phosphate buffer solutions (40mL) with same pH (7.4) at different temperatures 37 and 50°C for 6h. Following, 2 mL of the floating solution were withdrawn and substituted by the fresh buffer solution in each half-hour interval of the experiment time. The samples were determined at 270nm using UV–Vis spectrophotometer and eventually, total value of released BLT (Q_t) was computed using Eq. 9 [19].

$$Q_t = V_m C_t + \sum_{i=0}^{t-1} V_a C_i \quad (9)$$

In Eq. (9), V_m represents the volume of sample and V_a is the volume of the sample withdrawn. Also, the concentration of the drug at time "t" and "i" are shown by C_t and C_i ($i < t$), respectively. To determine the mechanism of BLT release from the synthesized SMNC, the drug release data were evaluated by different kinetic models as follows [20-26]:

$$Q_t = K_0 t \quad (10)$$

(pseudo – zero – order equation)

$$Q_t = (1 - e^{-k_1 t}) \quad (11)$$

(pseudo – first – order equation)

$$Q_t = K_H \sqrt{t} \quad (12)$$

(Higuchi equation)

$$\sqrt[3]{Q_0} - \sqrt[3]{Q_t} = K_{HC} t \quad (13)$$

(Hixson – Crowell equation)

$$Q_t = K_{KP} t^n \quad (14)$$

(Korsmeyer – Peppas equation)

In above equations, Q_t is the fraction of the BLT released at time "t"; the release constants are shown by k_0 , K_1 , K_H , K_{HC} , and K_{KP} . Besides, "n" in Eq. (14) presents the release exponent of Korsmeyer-Peppas model.

J. *BLT Release using NIR light irradiation*

In this study, in vitro BLT release from the produced SMNC was investigated at two different temperatures (37 and 50°C). To this aim, 10 mg of the loaded nano-carrier with BLT was immersed in ten transparent micro-tubes containing phosphate buffer solutions (1.5 mL) at pH 7.4. Immediately, the micro-tubes were exposed to the NIR light irradiation (at 808nm, 1.0 W/cm²) at predetermined time intervals (1, 3, 5, 10, and 15 min). Ultimately, the released BLT rate within the supernatants in the tubes was analyzed with the UV–Vis system at 270 nm. The mentioned procedures were repeated for a new series of samples in the absence of NIR light irradiation.

III. RESULTS AND DISCUSSION

A. *Characterization*

III.A.1. *Chemical structure and morphological characterization*

In this section, morphology, structure, and nanoparticles size of the pristine WS₂ and the synthesized SMNC were investigated via FE-SEM technique. In addition, EDX as a complementary characterization technique was used to determine the elemental content in the structure of the mentioned nanoparticles. According to Fig. 2(A), the unmodified WS₂ nanoparticles are mainly made up of layered and flake nano-sheets with a mean thickness between 20nm and 50 nm, which are stacked loosely. The findings were very similar to the observations of Wu et al. [27, 28]. The EDX curve of the WS₂ nanoparticles showed that these particles are composed of 84.26% of

tungsten (W) and 15.74% of sulfur (S). It is assumed that the presence of sulfur atoms on the nano-sheets facilitates the nano-sheets modification.

As can be seen in Fig. 2(B), the WS₂ nano-sheets structure has been preserved after the surface modification. It implies that the surface morphology of the nano-sheets remained approximately unchanged. Besides, the results showed that the mean thickness of the nano-sheets has increased up to 80nm after

modification, which could be attributed to successful synthesis of the polymer chains onto the nano-sheets. Likewise, the EDX pattern of the nano-carrier showed that the weight percentage of W (74.25%) and S (11.27%) has decreased significantly after modification. In contrast; the obtained data from EDX spectrum of the final nano-carrier verified the existence of elements such as C (6.08%), O (4.26%), and N (4.14%).

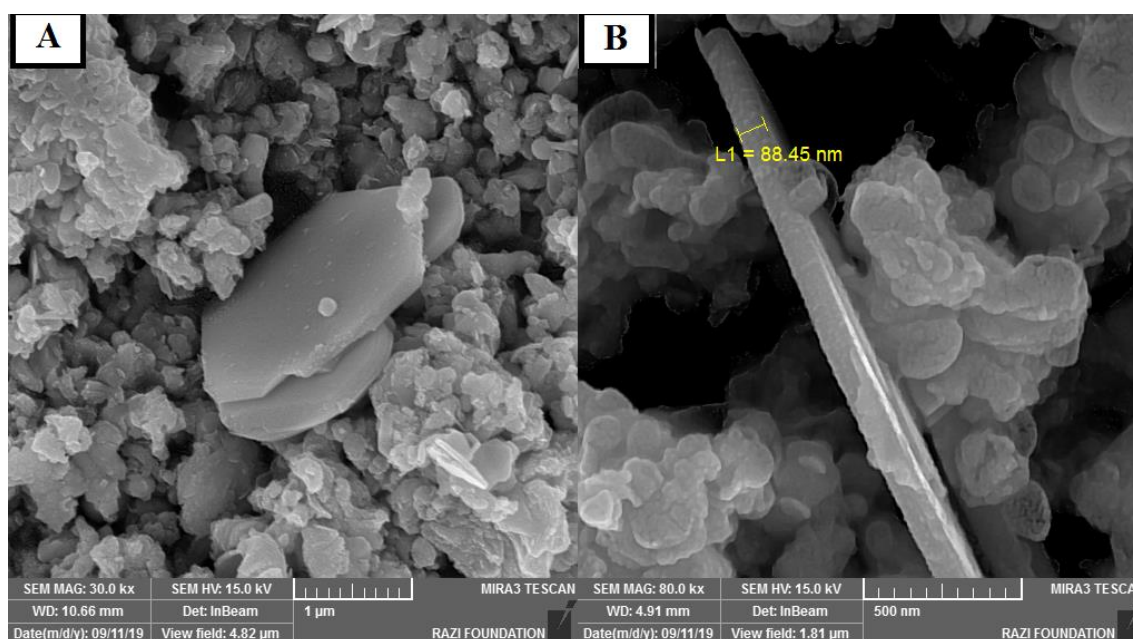


Fig. 2 FE-SEM images of the pristine WS₂ nano-sheets (A) and the produced SMNC (B).

B. Adsorption isotherms

Several well-known adsorption models were used to describe the liquid phase adsorption equilibria. The relevant isotherm outcomes for drug adsorption onto the synthesized SMNC are listed in Table 1. The Langmuir isotherm as the best known and simplest theoretical model is usually used for the monolayer adsorption onto the homogeneous surface with finite number of identical sites. In its formulation, If $R_L > 1$, it shows an unfavorable isotherm, $R_L = 1$ and $0 < R_L < 1$ indicate linear and favorable adsorption, respectively. Also, $R_L = 0$ means an irreversible adsorption. The Freundlich isotherm is an empirical equation and is most widely employed to explain non-ideal heterogeneous

adsorption in multiple adsorption layers. In Freundlich equation, if $0 < 1/n < 1$, it indicates a favorable adsorption. Temkin equation investigates the impact of some direct adsorbent-adsorbate interactive relation on adsorption isotherm.

Accordingly, this model expresses a linear decrease in the adsorption heat of all molecules in the layer with an increase in adsorbent surface coverage. Redlich-Peterson is an empirical equation integrate, which has incorporated features of both the Freundlich and Langmuir models. Besides, this model can be applied on homogeneous or heterogeneous surfaces. According to the calculated isotherm data in Table 1, higher correlation coefficient (R^2) was considered as a criterion for the acceptability of the isotherm model. Thus, the adsorption of BLT on the nano-carrier could well be fitted by the Langmuir model ($R^2 > 0.9981$); indicating the BLT adsorption is based on the monolayer adsorption. R_L was used to express the crucial features of the Langmuir model:

$$R_L = \frac{1}{(1 + K_L C_0)} \quad (15)$$

The R_L value calculated was less than one, demonstrating that the adsorption of BLT onto the nano-carrier is a favorable process. Also, the maximum adsorption capacity (q_{max}) was found 15.87 ($mg\ g^{-1}$). From the Freundlich model, the value of "n" as the heterogeneity factor was obtained more than 1, which verified a favorable and heterogeneous adsorption for BLT onto the synthesized nano-carrier.

Table 1 Isotherms parameters of BLT adsorption onto the produced SMNC (at 25°C)

Isotherm models	Quantity
Langmuir	
q_{max} ($mg\ g^{-1}$)	15.87
K_L ($L\ mg^{-1}$)	0.0824
R_L	0.2327
R^2	0.9981
Freundlich	
K_F ($mg\ g^{-1}$) ($L\ mg^{-1}$) ^{1/n}	1.1553
n	1.1204
R^2	0.9976

Temkin	
A ($L\ g^{-1}$)	3.4645
B	1.425
b ($J\ mol^{-1}$)	1739.5
R^2	0.8824
Redlich-Peterson	
A ($L\ g^{-1}$)	1.31
B	0.082
g ($L\ mg^{-1}$)	1.007
R^2	0.9962

C. Adsorption kinetics

Three kinetic models including first-order, second-order, and the intra-particle diffusion models were used for analyzing the adsorption function of BLT by the produced SMNC. The used models were evaluated based on correlation coefficient (R^2). As shown in Table 2, the R^2 value of the second-order model (0.9998) was higher than other two models and close to 1. Accordingly, the second-order model well fitted to the adsorption data.

Table 2 Kinetic parameters of BLT adsorption onto produced SMNC (at 25°C)

Kinetic models	
Pseudo-first-order	
q_e ($mg\ g^{-1}$)	0.4166
K_1 (min^{-1})	0.4076
R^2	0.9829
Pseudo-second-order	
q_e ($mg\ g^{-1}$)	2.8169
K_2 ($g\ mg^{-1}\ min^{-1}$)	4.2148
R^2	0.9998
Intra particle diffusion	
K_i ($mg\ g^{-1}\ min^{-1/2}$)	0.072
C_i ($mg\ g^{-1}$)	2.5748
R^2	0.9962

D. In vitro drug release

In vitro release behavior of BLT via dialyze bag method was examined in phosphate buffer (pH=7.4) as the simulated blood fluid at two different temperatures of 37 and 50°C. As can be seen from Fig. 4, the drug release rate at 50°C was achieved at a higher level than 37°C. In detail, 3.63% of BLT was released in the simulated fluid at 37°C within the first 1 h and 15.44% was released in remaining time (5 h). While, the profile of drug release at 50°C indicated a great percentage of BLT release in initial 1h (23.18%) and a medium growth rate

(63.71%) for the remaining time. It is inferred that the further shrinkage in thermo-sensitive polymer at higher temperature can lead to the further release of BLT from the nano-carrier. Hence, it can be concluded that the produced SMNC can be an attractive option for using in the targeted drug delivery systems.

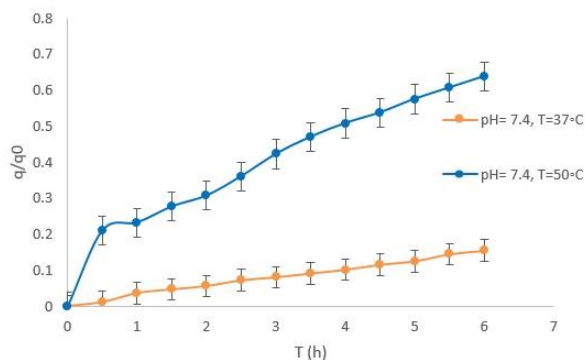


Fig. 4 The release profile of BLT at pH 7.4 and two different temperatures (37 and 50°C) (q/q_0 is the fraction of BLT release at time)

E. Drug release via NIR light

The drug release study from the synthesized SMNC was investigated in the presence and absence of NIR light irradiation at different time intervals (2-15 min). As shown in Fig. 5, the drug release rate under NIR light irradiation reached up to 100% over 10 min. As expected, the produced nano-carrier showed high response to NIR light irradiation due to the presence of thermo-sensitive polymer. In fact, when NIR light was emitted, the energy of NIR light irradiation was absorbed by the WS₂ nano-sheets and converted to the heat. Following, by increasing the local temperature and the shrinkage of the thermo-sensitive polymers, the loaded BLT was released.

The digital thermometer indicated an increase in solution temperature from 24 to 48°C in the exposure of NIR light irradiation for 15 min. Therefore, the synthesized nano-carrier not only can be used as an efficient drug delivery vehicle but also it could be employed for other applications like chemo-photothermal therapy due to rapid heating of the WS₂ nano-sheets by the NIR light irradiation. In addition, according to Fig. 5, a considerable decrease in drug

release rate was observed in the absence of NIR light irradiation from the nano-carrier. The results suggested that 18.96% of BLT was released in the absence of NIR light irradiation at the end of the experiment.

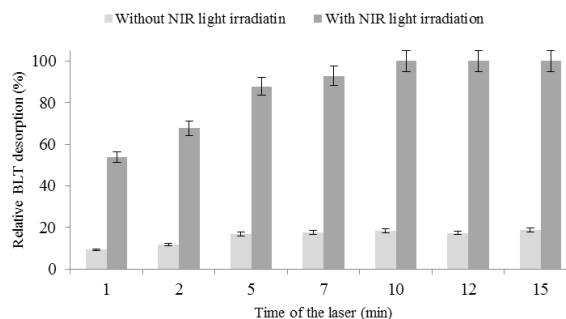


Fig. 5 BLT release percentage at 7.4 in the presence and absence of NIR light irradiation (at 25°C).

F. Kinetic models study for BLT release process

To describe the drug release from the produced SMNC, the in vitro drug release data were analyzed by several models and the results are presented in Table 3. According to the results obtained, the zero-order model described well the BLT release process due to the higher correlation coefficients (R^2) compared with other models. Specifically, the drug release mechanism was studied by using different “n” values in the Korsmeyer-Peppas model. According to the diffusion exponent 0.9 obtained for $R^2=0.9927$, the controlled diffusion mechanism followed from non-Fickian diffusion ($n > 0.5$) [29, 30].

Table 3 Release kinetic data of BLT from the produced SMNC.

Models Parameters	Zero-order		First-order		Higuchi		Hixson-Crowell		Korsmeyer- Peppas			
	$K_0(h^{-1})$	R^2	$K_0(h^{-1})$	R^2	$K_H(h^{1/2})$	R^2	$K_{HC}(h^{1/3})$	R^2	$K_{KP}(h^{-n})$	n	R^2	
pH=7.4	T=37°C	0.0244	0.9927	0.3713	0.8213	0.0792	0.978	-0.048	0.9158	0.1074	0.4	0.9692
		0.0792								0.0792	0.5	0.9780
		0.0605								0.0605	0.6	0.9847
		0.0473								0.0473	0.7	0.9893
		0.0376								0.0376	0.8	0.9921
		0.0302								0.0302	0.9	0.9932
	T=50°C	0.0244								0.0244	1	0.9927
		0.0672								0.0672	1.1	0.9895
		0.0825	0.992	0.2092	0.9641	0.2669	0.9748	0.0507	0.9773	0.3615	0.4	0.9642
		0.2669								0.2669	0.5	0.9748
		0.2041								0.2041	0.6	0.9828
		0.1596								0.1596	0.7	0.9883
								0.1268	0.8	0.9915		
								0.1019	0.9	0.9927		
								0.0825	1	0.9920		
								0.0199	1.1	0.9909		

IV. CONCLUSIONS

In this study, smart thermo-sensitive polymeric chains were successfully grafted onto the WS₂ nano-sheets as a nano drug vehicle for delivery of bicalutamide. The analysis results from FESEM-EDX, FT-IR, XRD, and TGA confirmed the grafted polymer networks onto the surface of WS₂ nano-sheets. The evaluation of adsorption isotherm models revealed that the Langmuir model fitted well to the adsorption of BLT ($R^2 = 0.9981$). Also, the kinetic data obeyed the second-order model with $R^2 = 0.9998$. In vitro release of BLT from the produced nano-carrier at 37°C (15.44%) was slower than the drug release at 50°C (63.71%) in the simulated blood fluid within 6 h. The results of the in vitro drug release of BLT under NIR light irradiation (at 808 nm, 1.0 W cm²) and without NIR irradiation were 100% and 18.96% , respectively (at pH = 7.4). Besides, the assessment of the drug release models demonstrated that the kinetic data obeyed the zero-order model. The diffusion exponent value (n) obtained from Korsmeyer–Peppas model verified that the drug release mechanism is of non-Fickian diffusion ($n > 0.5$).

REFERENCES

- [1] E. D. Crawford, "Epidemiology of prostate cancer," *Urology*. Vol. 62, pp. 3-12, 2003.
- [2] I. D. Cockshott, "Bicalutamide, Clinical pharmacokinetics," Springer, vol. 43, pp. 855–878, 2004.
- [3] S. Senapati, A. Kumar Mahanta, S. Kumar, and P. Maiti, "Controlled drug delivery vehicles for cancer treatment and their performance," *Signal Transduct Target Ther*. Vol. 3, pp. 1-7, 2018.
- [4] Y. Lee and D. Thompson, "Stimuli-responsive liposomes for drug delivery," *Wiley Interdisciplinary Reviews: Nanomedicine and Nanobiotechnology*, vol. 9, pp. 1450 (1-76), 2017.
- [5] W. Paul and C. P. Sharma, "Inorganic nanoparticles for targeted drug delivery," *Biointegration of Medical Implant Materials*, vol. 333, pp. 204-235, 2020.
- [6] J.P. Raval, P. Joshi, and D.R. Chejara, "Carbon nanotube for targeted drug delivery," *Applications of nanocomposite Materials in drug delivery: Elsevier*, vol. 203, pp. 203-216, 2018.
- [7] Q. Zhou, L. Zhang, T.H. Yang, and H. Wu, "Stimuli-responsive polymeric micelles for drug delivery and cancer therapy,"

- International journal of nanomedicine. Vol.13 pp. 2921–2942, 2018.
- [8] M. Wu and S. Huang, “Magnetic nanoparticles in cancer diagnosis, drug delivery and treatment,” *Molecular and clinical oncology*. Vol. 7, pp. 738–746, 2017.
- [9] Y. Yong, L. Zhou, Zh. Gu, L. Yan, G. Tian, X. Zheng, X. Liu, X. Zhang, J. Shi, W. Cong, W. Yin, and Y. Zhao “WS 2 nanosheet as a new photosensitizer carrier for combined photodynamic and photothermal therapy of cancer cells,” *Nanoscale*. Vol. 6, pp. 10394-10403, 2014.
- [10] Q. Liu, Ch. Sun, Q. He, A. Khalil, T. Xiang, D. Liu, Y. Zhou, J. Wang and L. Song, “Stable metallic 1T-WS 2 ultrathin nanosheets as a promising agent for near-infrared photothermal ablation cancer therapy,” *Nano Research*. Vol. 8, pp. 3982–3991, 2015.
- [11] M.J. Khodabakhshi, H. Ahmad Panahi, H. A. Panahi, E. Kono, A. Feizbakhsh, and Salimeh Kimiagar, “NIR-triggered drug delivery system based on Fe₃O₄-MoS₂ core-shell grafted poly (N-vinylcaprolactam): isotherm and kinetics studies,” *Polymer-Plastics Technology and Materials*. Vol.60, pp. 1247-1260, 2021.
- [12] H. Freundlich, “Über die adsorption in lösungen,” *Zeitschrift für physikalische Chemie*. Vol. 57, pp. 385-490, 1907.
- [13] I. Langmuir, “The adsorption of gases on plane surfaces of glass, mica and platinum,” *Journal of the American Chemical society*. Vol. 40, pp. 1361–1403, 1918.
- [14] M. Temkin, "The kinetics of some industrial heterogeneous catalytic reactions," *Advances in Catalysis*, vol. 28, pp. 173-291, 1979.
- [15] O. Redlich and D. L. Peterson, “A useful adsorption isotherm,” *Journal of physical chemistry*. Vol. 63, pp. 1024, 1959.
- [16] Y.-S. Ho and G. McKay, “Pseudo-second order model for sorption processes,” *Process biochemistry*. Vol. 34, vol. 451-465, 1999.
- [17] S. K. Lagergren, “About the theory of so-called adsorption of soluble substances,” *Sven. Vetenskapsakad. Handlingar*. Vol. 24, pp. 1-39, 1898.
- [18] W. J. Weber Jr and J. C. Morris, “Kinetics of adsorption on carbon from solution,” *Journal of the sanitary engineering division*. Vol. 89, pp. 31-59, 1963.
- [19] Sh. Padash Hooshyar, R. Zafar Mehrabian, H. Ahmad Panahi, M. Habibi Jouybari, and H. Jalilian, “Synthesis and characterization of magnetized-PEGylated dendrimer anchored to thermosensitive polymer for letrozole drug delivery,” *Colloids and Surfaces B: Biointerfaces*. Vol. 176, pp. 404-411, 2019.
- [20] M. Gibaldi and S. Feldman, “Establishment of sink conditions in dissolution rate determinations. Theoretical considerations and application to nondisintegrating dosage forms,” *Journal of pharmaceutical sciences*. Vol. 56 pp.1238-1242, 1967.
- [21] T. Higuchi, “Rate of release of medicaments from ointment bases containing drugs in suspension,” *Journal of pharmaceutical sciences*, Vol. 50, pp. 874-875, 1961.
- [22] T. Higuchi, “Mechanism of sustained-action medication. Theoretical analysis of rate of release of solid drugs dispersed in solid matrices,” *Journal of pharmaceutical sciences*, Vol. 52, pp. 1145-1149, 1963.
- [23] A. Hixson and J. Crowell, “Dependence of reaction velocity upon surface and agitation,” *Industrial and Engineering Chemistry*. Vol. 23, pp. 923–931, 1931.
- [24] C.G. Varelas, D.G. Dixon, and C.A. Steiner, “Zero-order release from biphasic polymer hydrogels,” *Journal of controlled release*. Vol. 34, pp. 185-192, 1995.
- [25] J. G. Wagner, “Interpretation of percent dissolved-time plots derived from in vitro testing of conventional tablets and capsules,” *Journal of pharmaceutical sciences*, Vol. 58, pp.1253-1257, 1969.
- [26] R.W. Korsmeyer, R. Gurny, E. Doelker, P. Buri, and N. A. Peppas, “Mechanisms of solute release from porous hydrophilic polymers,” *International journal of pharmaceutics*. Vol.15, pp. 25-35, 1983.
- [27] Z. Wu, D. Wang, X. Zan, and A. Sun, “Synthesis of WS₂ nanosheets by a novel mechanical activation method,” *Materials Letters*. vol. vol. 64, pp. 856-858, 2010.
- [28] A. Bohloli, M.D. Asli, E. Moniri, and A.B. Gh, “Modification of WS 2 nanosheets with beta-cyclodextrone and N-isopropylacrylamide polymers for tamoxifen adsorption and investigation of in vitro drug release,” *Research on Chemical Intermediates*. Vol. 47, pp. 1955–1978, 2021.

[29] N. Peppas, "Analysis of Fickian and non-Fickian drug release from polymers," *Pharmaceutica Acta Helvetiae*. Vol. 60, pp. 110-111, 1985.

[30] P. L. Ritger and N. A. Peppas, "A simple equation for description of solute release II. Fickian and anomalous release from swellable devices," *Journal of controlled release*. Vol. 5, pp. 37-42, 1987.

THIS PAGE IS INTENTIONALLY LEFT BLANK.